Biomedical Journal 47 (2024) 100613

Contents lists available at ScienceDirect

Biomedical Journal

journal homepage: www.elsevier.com/locate/bj

Original Article

Repeated administration of adipose-derived mesenchymal stem cells added on beneficial effects of empagliflozin on protecting renal function in diabetic kidney disease rat

Chih-Chao Yang [a], Yi-Ling Chen [b], Pei-Hsun Sung [b,c,d], John Y. Chiang [e,f], Chih-Hung Chen [g], Yi-Chen Li [b,h,i,j,1,**], Hon-Kan Yip [b,c,d,k,l,1,*]

[a] Division of Nephrology, Department of Internal Medicine, Kaohsiung Chang Gung Memorial Hospital and Chang Gung University College of Medicine, Kaohsiung, Taiwan
[b] Division of Cardiology, Department of Internal Medicine, Kaohsiung Chang Gung Memorial Hospital and Chang Gung University College of Medicine, Kaohsiung, Taiwan
[c] Center for Shockwave Medicine and Tissue Engineering, Kaohsiung Chang Gung Memorial Hospital, Kaohsiung, Taiwan
[d] Institute for Translational Research in Biomedicine, Kaohsiung Chang Gung Memorial Hospital, Kaohsiung, Taiwan
[e] Department of Computer Science & Engineering, National Sun Yat-Sen University, Kaohsiung, Taiwan
[f] Department of Healthcare Administration and Medical Informatics, Kaohsiung Medical University, Kaohsiung, Taiwan
[g] Divisions of General Medicine, Department of Internal Medicine, Kaohsiung Chang Gung Memorial Hospital and Chang Gung University College of Medicine, Kaohsiung, Taiwan
[h] Clinical Medicine Research Center, National Cheng Kung University Hospital, College of Medicine, National Cheng Kung University, Tainan, Taiwan
[i] Center of Cell Therapy, National Cheng Kung University Hospital, College of Medicine, National Cheng Kung University, Tainan, Taiwan
[j] Institute of Clinical Medicine, College of Medicine, National Cheng Kung University, Tainan, Taiwan
[k] Department of Nursing, Asia University, Taichung, Taiwan
[l] Department of Medical Research, China Medical University Hospital, China Medical University, Taichung, Taiwan

ARTICLE INFO

Keywords:
Diabetic kidney disease
Renal function
Inflammation
Oxidative stress

ABSTRACT

Background: Diabetic kidney disease (DKD) is one of the most significant public health burdens worldwide. This study explored the renal protections of combined adipose-derived mesenchymal stem cells (ADMSCs) and empagliflozin (EMPA) in DKD rats.

Methods: Adult-male-SD rats were equally allocated into group 1 (sham-operated-control), group 2 (DKD), group 3 (DKD + EMPA/20 mg/kg/day since day-14 after CKD-induction), group 4 [DKD + ADMSCs (6.0×10^5/intrarenal-arterial-injection/post-day-28, followed by 1.2×10^6/intravenous injection post-days 35 and 42 after CKD-induction, i.e., defined as repeated administration)] and group 5 (DKD + ADMSCs + EMPA) and kidney was harvested post-day-60 CKD-induction.

Results: The result showed that the blood sugar and circulatory levels of BUN/creatinine and the ratio of urine protein/creatinine at day 60 were greatly increased in group 2 as compared the SC (i.e., group 1), significantly increased in groups 3 and 4 than in groups 5, but these parameters showed the similar manner in groups 3 and 4, except for blood sugar that was significantly lower in group 3 than in group 4 (all $p < 0.0001$). The protein levels of inflammation (NF-κB/FNF-α/MMP-9)/oxidative-stress (NOX-1/NOX-2/oxidized protein/p22-phox)/apoptosis (cleaved-caspase-3/cleaved-PARP/mitochondrial-Bax)/fibrosis (TGF-β/Smad 3)/mitochondrial/DNA-damaged (p-DRP1/γ-H2AX) biomarkers revealed a similar manner of creatinine level among the groups (all $p <$ 0.0001). Kidney injury score/fibrotic area/oxidative-stress score (8-OHdG) and cellular levels of kidney-damaged biomarkers (KIM-1/γ-H2AX) showed a unanimous manner. In contrast, the cellular expressions of

Peer review under responsibility of Chang Gung University.

* Corresponding author. Division of Cardiology, Department of Internal Medicine, Kaohsiung Chang Gung Memorial Hospital, 123, Ta Pei Rd., Niao Sung Distr., Kaohsiung 83301, Taiwan. Tel.: +886 7 7317123#2363.

** Corresponding author. Clinical Medicine Research Center, National Cheng Kung University Hospital, 138, Shengli Rd., Tainan 70403, Taiwan. Tel.: +886 6 2353535#4207.

E-mail addresses: ryichenli@gmail.com, n152328@mail.hosp.ncku.edu.tw (Y.-C. Li), han.gung@msa.hinet.net, hkyip@cgmh.org.tw (H.-K. Yip).

[1] These authors jointly supervised this work.

https://doi.org/10.1016/j.bj.2023.100613
Received 26 October 2022; Accepted 5 June 2023
Available online 22 June 2023

podocyte components (ZO-1/synaptopodin) revealed an antithetical manner of creatinine among the groups (all $p < 0.0001$).
Conclusion: Combined ADMSCs-EMPA was superior to just one therapy for protecting kidney function and ultrastructural integrity in DKD rodents.

Chronic kidney disease (CKD) has emerged as one of the most significant public health burdens worldwide. Among the etiologies, diabetes is the most common cause of CKD, i.e., diabetic CKD called DKD [1]. WHO has estimated that globally, 422 million adults were living with diabetes in 2014, and the number is expected to rise to 700 million by 2045 [2]. Additionally, the prevalence of DKD has been rapidly increasing by almost 12% from 1990 to 2013 [1,3]. Notably, cardiovascular disease mortality is the most excess risk of death for patients with DKD [4]. Currently, DKD (43.2%) is the primary underlying renal disease of end-stage renal disease (ESRD) in Asia [5] Accordingly, to attenuate the impact of DKD on patients' unfavorable outcomes and reduce medical costs, developing an innovative treatment with safety and efficacy for renal protection in diabetic patients is crucial and urgently needed.

Basic research has emphasized that chronic hyperglycemia commonly causes mitochondrial superoxide overproduction, which, in turn, makes the kidney more susceptible to damage, such as acute kidney injury (AKI) [6,7]. Additionally, persistent hyperglycemia (i.e., diabetes mellitus) certainly alters vasoactive regulators of afferent and efferent arteriolar tone, resulting in increasing glomerular capillary hydraulic pressure, hyper-perfusion, and hyperfiltration [8,9]. Of importance is that the sodium-glucose cotransporter 2 (SGLT2) enzyme, which is commonly upregulated by these pathophysiological phenomena, is thought to play an essential role in tubuloglomerular feedback signalings, leading to inappropriate afferent vasodilatation [10]. The consequent intraglomerular hypertension and hyperfiltration promote deterioration of renal function in the setting of DKD, eventually increasing overall long-term morbidity and mortality [11].

Interestingly, a study has shown that empagliflozin (EMPA) (i.e., SGLT2 inhibitor) inhibited SGLT2 release from proximal tubular epithelial cells [12]. Clinical trials [13–15] have further demonstrated that SGLT2 inhibitors were associated with a lower rate of adverse renal outcomes. It is also well recognized that the pathogenesis of cardiorenal syndrome (CRS), which included upregulation of reactive oxygen species (ROS), mitochondrial dysfunction, and systemic inflammation [12], was reversed by SGLT2 inhibitors [16,17] resulting in preserving the residual renal function [18].

Overwhelming evidence has illustrated that mesenchymal stem cells (MSCs), particularly those of adipose-derived MSCs (i.e., ADMSCs), not only encompass the capability of assuaging inflammation and ROS but also contain capacities of tissue rebirth and immunoregulation [19–25]. Additionally, copious animal model studies and a few clinical trials have shown that cell-based therapy furnished significant advantages for settings of CKD, acute kidney injury, or CRS [26–30]. Furthermore, our recent studies have proved that cell-based therapy endured a dose-dependent effect (i.e., a single dose was inferior to two doses) on improving the outcomes in damaged organs [31,32]. Based on these subjects [12–24,26–34], it is reasonable to believe that repeated doses of ADMSCs administration might facilitate the therapeutic potential of EMPA on DKD rodents.

Materials and methodologies

Ethical issues

The formalities of animal investigations were authorized by the Committee at Kaohsiung Chang Gung Memorial Hospital (Affidavit of Approval of Animal Use Protocol No. 2020092205), following the Guide for the Care and Use of Laboratory Animals, and housed in an AAALAC-approved animal facility in our hospital with suitable temperature and light cycles (24 °C and 12/12 light cycle) for animals.

The CKD induction, animal groups, DKD induction, blood sugar record, and definition of diabetes mellitus (DM)

Adult male SD rats were used in our study. The program of CKD induction has been mentioned in our previous report [33]. Briefly, animals in all groups were anesthetized by inhalational 2.0% isoflurane for midline laparotomies. While the sham-operated control (SC) rats accepted laparotomy only, the CKD was conducted in the animals of CKD groups using right nephrectomy plus arterial ligation of the upper 2/3 (upper and middle poles) blood conveyances of the left kidney, leaving the lower 1/3 part of (lower pole) kidney with normal blood flow.

The DM induction was created on the 7th day after CKD induction, as described by our recent study [34]. In detail, streptozotocin (STZ) (30 mg/kg) and aminoguanidine (180 mg/kg) [i.e., to protect those of the beta cells (β-cells) in islets of the pancreas for avoiding complete destruction, similar to a set of type II DM] were intraperitoneally delivered at the 7th day following CKD induction and carried on once only, resulting in a DKD animal model. The reason and dosage of aminoguanidine (AMG) to be applied in the current animal model investigation were according to the previous report [35]. Since the result from this investigation [35] revealed that AMG was able to provoke the biosynthesis and release of insulin, resulting in inhibition of the advanced glycosylation end products (AGEs) formation and accumulation in islets as well as alleviating the glucotoxicity for the β-cells.

After completing the induction of DKD, the rodents were equally divided into group 1 (SC), group 2 (DKD), group 3 (DKD + EMPA/20 mg/kg/day since day 14 after CKD induction), group 4 [DKD + ADMSCs (6.0×105 by intrarenal arterial injection at 28th day after CKD induction, followed by 1.2×106 cell by intravenous administration at 35th and 42nd days after CKD induction)], and group 5 (DKD-ADMSC-EMPA). The kidney was harvested from each animal by day 60 CKD induction.

The dosage of the ADMSCs utilization was according to our previous reports [31,34] with minimal modification. Additionally, by day 28 after CKD induction [refer to Supplementary Fig. 1], the laparotomy was conducted again. The renal artery was isolated by visual observation, followed by ADMSCs inside a 30# needle carefully and slowly administered into the renal artery. After the ADMSCs administration, the needle was pulled out, and careful compression was applied to the needle wound until the bleeding was stopped.

Monitoring the circulatory blood sugar level and definition of DM were based on our previous study [29,34]. In detail, the circulatory sugar level of each animal was assessed at 8:00–9:00 a.m. using a blood glucose monitor (ACCU-CHEK-Active; Roche) on day 14 and day 60 after CKD induction. After STZ treatment for 7 days, we detected the blood glucose levels and defined ≥250 mg/dL as a successful DM induction.

Preparing allogenous ADMSCs for different points of treatment

To isolate adipose tissue for ADMSCs, culture was carried out in additional 24 animals (i.e., the donors of allogenous ADMSCs) for those of groups 4 and 5 (i.e., called recipients). Adipose tissues situated in the epididymis and abdominal areas were carefully isolated according to our previous reports [24,28] at different time intervals of treatment. Cell

culture was performed in Dulbecco's modified Eagle's medium (DMEM)-low glucose medium containing 10% FBS for at least 14 days. Roughly 2.5–3.5 × 106 ADMSCs were gathered from each animal at this time interval.

Examination of circulatory blood urine nitrogen (BUN) and creatinine levels

To elucidate if the CKD animal model was successfully established and the effect of ADMSCs treatment on preserving the renal function, blood-sample collections were serially performed prior to and after the CKD induction (i.e., prior to and at days 14, 28, and 60 after CKD induction prior to the animals were sacrificed). Standard laboratory methods calculated circulatory levels of creatinine and BUN.

Collecting 24 h urine for the serial changes of the ratio of urine protein to creatinine

Our previous report has written the methodology for assessing this parameter [33]. To collect 24 h urine for the study, animals in each group were arranged in a metabolic cage for 24 h with a free intake of food and water. Urine in 24 h was collected in all rats before and at days 14, 28, and 60 after CKD induction to examine the ratio of urine protein to urine creatinine.

Measuring the time courses of the renal artery resistive index (RARI)

The RI is an essential and reliable factor for determining renal arterial resistance in variable kidney diseases, such as CKD or DKD settings. By using the ultrasound machine (Vevo 2100, VisualSonics), an expert animal ultrasound specialist measured two parameters of the renal artery, including (1) peak systolic blood velocity (PSV) and (2) lowest diastolic blood velocity (LDV). Thus, the calculation formula was defined as RI = (PSV-LDV)/PSV.

Microstructural examination for renal injured scoring by day 60 after CKD induction

The methods for determining the protein levels of investigated biomarkers have been depicted in our previous studies. The kidney histopathological-injury score was analyzed in a blinded fashion, as we have previously described [36]. Briefly, all rats' left kidney specimens were prepared well and embedded in paraffin, sectioned at 4 μm, and stained by H & E for the light microscope. Within detecting 10 randomly chosen non-overlapping fields (200x) for each animal, the score indicated the percentages including 1) grading of tubular necrosis; 2) loss of brush border; 3) cast formation; and 4) tubular dilatation as follows: 0 (none), 1 (≤10%), 2 (11–25%), 3 (26–45%), 4 (46–75%), and 5 (≥76%).

Western blot analysis of left kidney specimens

The methods for determining the protein levels of investigated biomarkers have been depicted in our previous studies [37]. Briefly, equal amounts (50 μg) of protein extracts were loaded and separated by SDS-PAGE using acrylamide gradients. The membranes were incubated with the indicated primary antibodies to detect the parameters' amount [matrix metalloproteinase 9 (MMP9) (1: 1000, Abcam), phosphorylated nuclear factor p–NF)–kB (1: 1000, Cell Signaling), NOX-1 (1: 1000, Sigma), NOX-2 (1: 1000, Sigma), cleaved poly ADP ribose polymerase (PARP) (1: 1000, Cell Signaling), mitochondrial Bax (1: 1000, Abcam), tumor necrosis factor (TNF)-α (1: 1000, Cell Signaling), P22 phox (1: 1000, Abcam), p-Smad 3 (1: 1000, Cell Signaling), transforming growth factor (TGF)-β (1:1000, Abcam), p-Smad 1/5 (1: 1000, Cell Signaling), bone morphogenetic protein (BMP)2 (1: 1000, Abcam), phosphorylated dynamin-related protein 1DRP1 (1: 1000, Cell Signaling), γ-H2AX (1: 1000, Cell Signaling), Atg 5 (1: 1000, Cell Signaling), cleaved caspase 3 (1: 1000, Cell Signaling), oxidized protein (1:100, Millipore) and Actin (1: 10,000, Chemicon)] for 1 h at room temperature. Horseradish peroxidase-conjugated secondary antibodies were further incubated for 1 h at room temperature and performed by enhanced chemiluminescence (ECL; Amersham Biosciences, Amersham, UK), followed by exposure to Biomax L film (Kodak, Rochester, NY, USA). For the quantifications of protein expressions, ECL signals were evaluated using Labwork software (UVP, Waltham, MA, USA).

Immunohistochemical (IHC) and immunofluorescent (IF) studies

The procedures and protocols for IHC and IF examinations were based on our previous reports [33,38]. Briefly, IF stain was conducted for the analyses of the specific parameters [8-hydroxy-2-deoxyguanosine (8-OHdG) (1: 500, Abcam), ZO-1 (1: 200, Abcam), kidney injury molecule (KIM-1) (1:400, Novus), and Synaptopodin (1:500, Santa Cruz)]. Respective primary antibody was used with irrelevant antibodies as controls. Three sections of kidney specimens were assessed in each animal. Three randomly selected microscope HPFs (200x for IHC and IF studies) were examined on each slide for quantification. The mean number per HPF for each rat was calculated by summation of all numbers divided by 9.

An IHC-based scoring system was adopted for semi-quantitative analysis of 8-OHdG in the kidney as a percentage of positive cells in a blinded fashion [score of positively-stained cell: 0 = negative staining; 1 = 1–15%; 2 = 16–25%; 3 = 26–50%; 4 = 51–75%; and 5 = 76–100% per high-power field (HPF)]. Additionally, an IF-based scoring system was adopted for the semi-quantitative analysis of KIM-1 in the kidney that was identical to the method outlined above for the analysis of 8-OHdG.

Moreover, the fluorescence intensities of ZO-1 and synaptopodin wereobserved by fluorescence microscope (Olympus BX51: fluorescence imaging system of OLYMPUS cellSens Standard 1.17) and converted to arbitrary units (AU) by ImageJ software 1.53 edition. For quantification, fluorescence intensity was used to confirm the area of integrated intensity and the selected mean gray value. Fluorescence intensity represents the integrated density, which was area x average fluorescence of background readings.

Statistical analysis

Quantitative parameters were shown as mean ± SD. The statistical analyses were performed using SPSS 18 (IBM) software and GraphPad Prism (GraphPad Software v.8.0). ANOVA was calculated and analyzed, followed by Bonferroni multiple comparison post hoc tests for comparing variables among groups. The probability value < 0.05 was considered as the statistical significance.

Results

The procedure and protocol of CKD and DKD inductions, the time points of treatment, and mortality rate of animals among the groups

[Supplementary Fig. 1] illustrates the time points of CKD and DKD inductions. By days 60 after CKD (i.e., the end of the study period), the animals in each group were euthanized prior to abdominal ultrasound examination, and the kidney in each animal was harvested for individual study.

[Supplementary Table 1] demonstrated the number of animals to be utilized, the time point of animal death, and the accumulated survival rate at the end of the study period. By the end of the study period, the accrued survival rate was 100.00% in group 1 (SC), 43.75% in group 2 (DKD), 68.75% in group 3 (DKD + EMPA), 75.00% in group 4 (DKD + ADMSCs), and 68.75% in group 5 (DKD + ADMSC + EMPA), respectively. The statistically significant difference in accumulated mortality rate was only present in SC group vs. group 2 ($p < 0.01$), indicating not

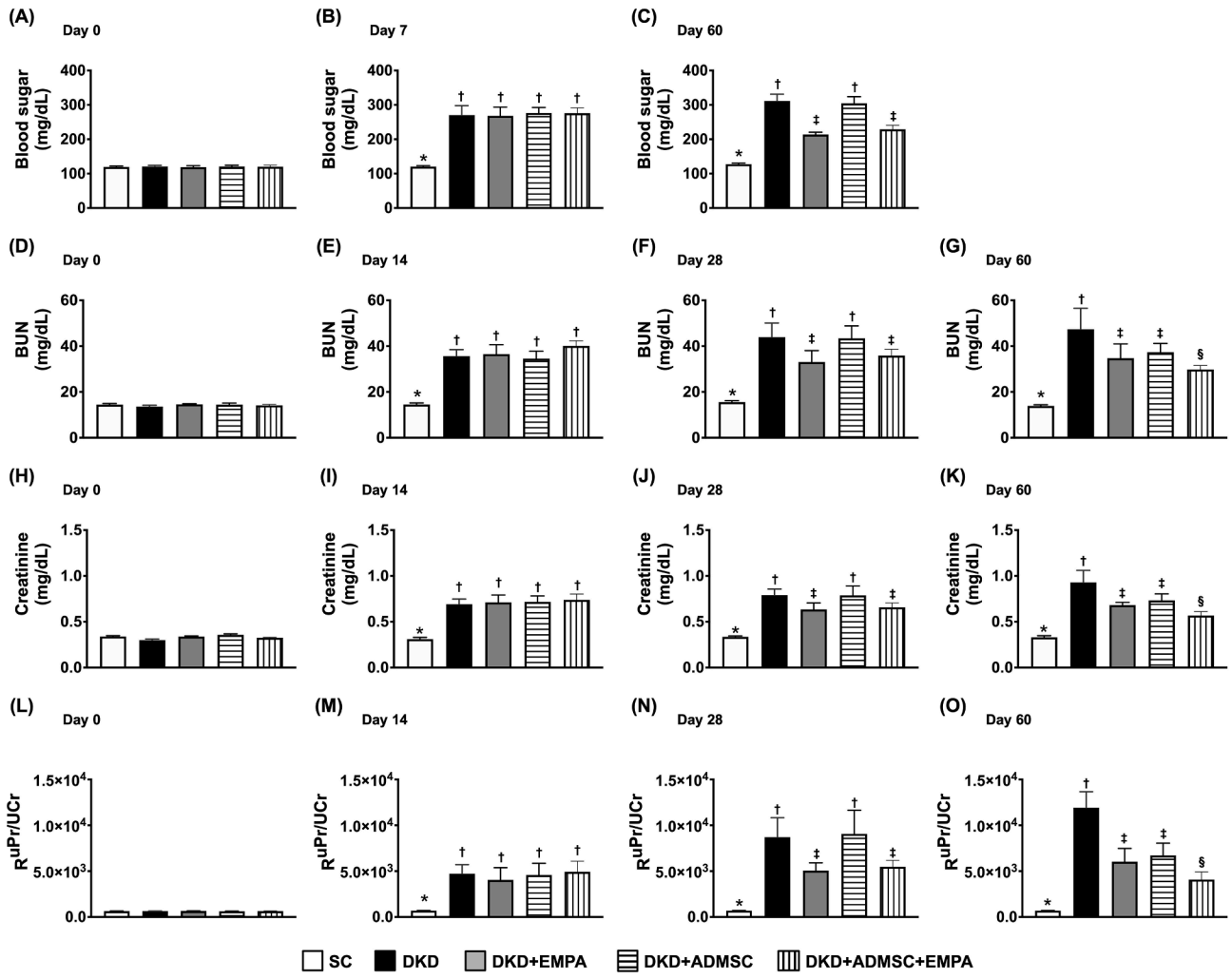

Fig. 1. Time courses of the circulating levels of blood sugar, blood urine nitrogen, and creatinine, and the ratio of urine protein to urine creatinine (A) Circulating blood sugar level at day 0, $p > 0.5$. **(B)** Circulating level of blood sugar at day 7 after streptozotocin treatment, * vs. other groups with different symbols (†, ‡), $p < 0.0001$. **(C)** Circulating level of blood sugar at day 60 after CKD induction, * vs. other groups with different symbols (†, ‡), $p < 0.0001$. **(D)** Circulatory level of BUN at day 0, $p > 0.5$. **(E)** Circulatory level of BUN at day 14 after CKD induction, * vs. †, $p < 0.0001$. **(F)** Circulatory level of BUN at day 28 after CKD induction, * vs. other groups with different symbols (†, ‡), $p < 0.0001$. **(G)** Circulatory level of BUN at day 60 after CKD induction, * vs. other groups with different symbols (†, ‡, §), $p < 0.0001$. **(H)** Circulatory level of creatinine at day 0, $p > 0.5$. **(I)** Circulatory level of creatinine at day 14 after CKD induction, * vs. †, $p < 0.0001$. **(J)** Circulatory level of creatinine at day 28 after CKD induction, * vs. other groups with different symbols (†, ‡), $p < 0.0001$. **(K)** Circulatory level of creatinine ay day 60 after CKD induction, * vs. other groups with different symbols (†, ‡, §), $p < 0.0001$. **(L)** Ratio of urine protein to urine creatinine ($R^{UPr/UCr}$) at day 0, $p > 0.5$. **(M)** $R^{UPr/UCr}$ at day 14 after CKD induction, * vs. †, $p < 0.0001$. **(N)** $R^{UPr/UCr}$ at day 28 after CKD induction, * vs. other groups with different symbols (†, ‡), $p < 0.0001$. **(O)** $R^{UPr/UCr}$ at day 60 after CKD induction, * vs. other groups with different symbols (†, ‡, §), $p < 0.0001$. All statistical analyses were performed by one-way ANOVA, followed by Bonferroni multiple comparison post hoc test (n = 7 to 11 for each group). Symbols (*, †, ‡, §) indicate significance (at 0.05 level).
Abbreviations: CKD : chronic kidney disease; BUN : blood urea nitrogen; SC : sham-operated control; DKD : diabetic kidney disease; EMPA : empagliflozin; ADMSC : adipose-derived mesenchymal stem cell.

only EMPA but also ADMSCs therapy prolonged survivals and provided the positive outcomes in DKD rats.

Time courses of the circulating levels of blood sugar, BUN, and creatinine, and the ratio of urine protein to urine creatinine

The baseline level of circulatory blood sugar did not differ among the groups [Fig. 1A]. However, by day 7 (i.e., day 14 after CKD induction) after STZ, the blood sugar was significantly higher in groups 2 to 5 (i.e., mean value > 250 mg/dL in these 4 groups) than in that of the SC group [Fig. 1B]. This finding was defined as a successful DM induction. Additionally, by day 60 after CKD (i.e., just equal to day 53 after successful DM induction), the circulatory level of blood sugar was lowest in SC group, most significantly increased in group 2 and significantly increased in group 4 than in groups 3 and 5, but it did not differ between groups 3 and 5 [Fig. 1C].

Next, to elucidate the impact of ADMSCs-EMPA on safeguarding the residual renal function in DKD animals, the time courses of blood samplings were collected for measuring the circulatory levels of BUN and creatinine, and the urine was collected for assessment of the ratio of urine protein to urine creatinine. As we expected, the baseline levels of these three parameters were similar among the groups [Fig. 1D, H, L]. However, by day 14 after CKD induction, these three parameters were significantly higher in groups 2 to 5 as compared with the SC group, but they did not differ among the latter 4 groups [Fig. 1E, I, M]. Additionally, by day 28, these three parameters were significantly higher in groups 2 to 5 as compared to the SC group, and considerably higher in groups 2 and 4 than in groups 3 and 5, but they were similar between the groups 2 and 4 and between the groups 3 and 5 [Fig. 1F, J, N]. Furthermore, by the end of the study period (i.e., at day 60 after CKD

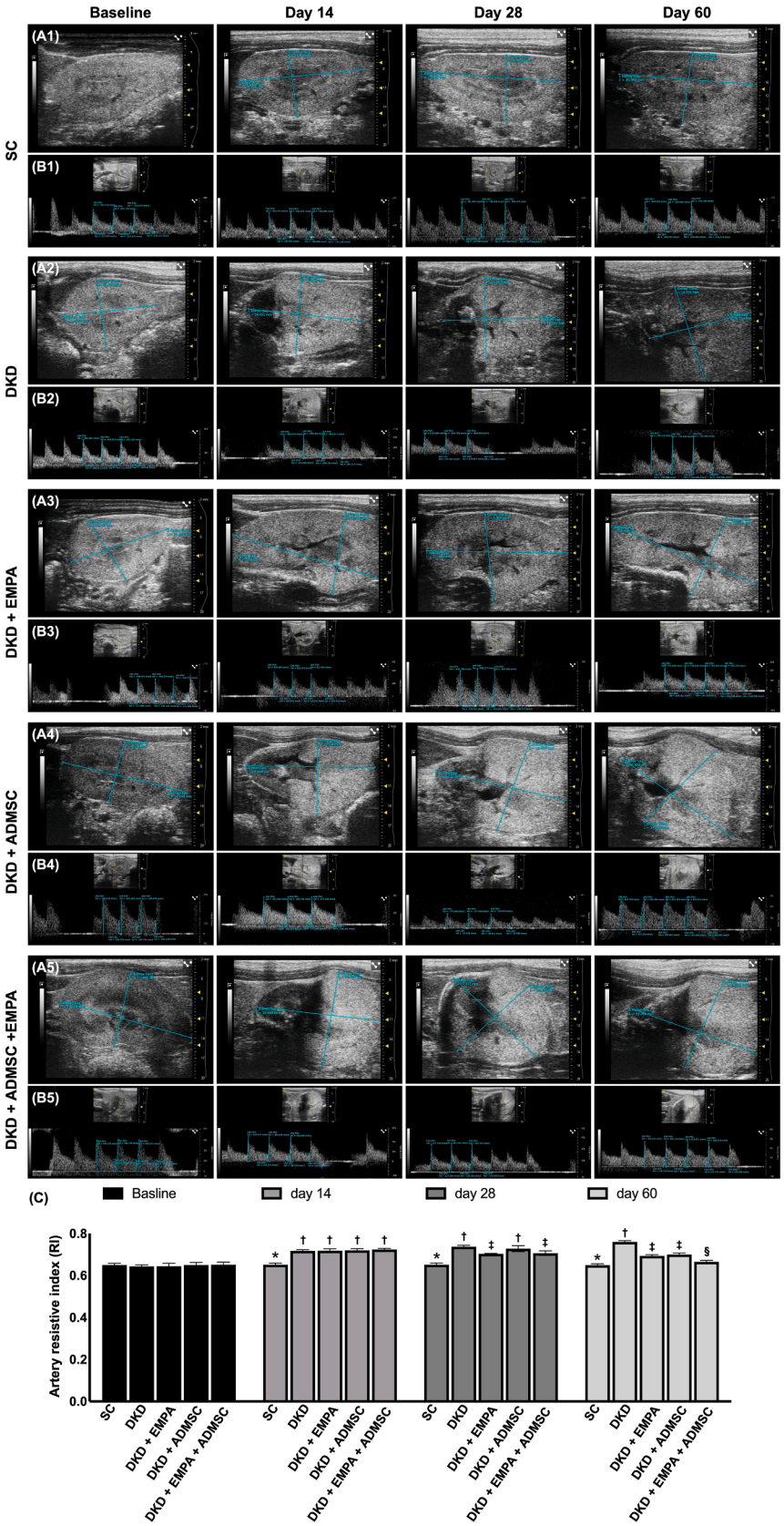

Fig. 2. Serial changes of renal artery resistive index (RARI) (A) The RARI at day 0, $p > 0.5$. **(B)** The RARI at day 14 after CKD induction, * vs. †, $p < 0.0001$. **(C)** The RARI at day 28 after CKD induction, * vs. other groups with different symbols (†, ‡), $p < 0.0001$. **(D)** The RARI at day 60 after CKD induction, * vs. other groups with different symbols (†, ‡, §), $p < 0.0001$. All statistical analyses were performed by one-way ANOVA, followed by Bonferroni multiple comparison post hoc test (n = 7 to 11 for each group). Symbols (*, †, ‡, §) indicate significance (at 0.05 level).

Abbreviations: CKD : chronic kidney disease; SC : sham-operated control; DKD : diabetic kidney disease; EMPA : empagliflozin; ADMSC : adipose-derived mesenchymal stem cell.

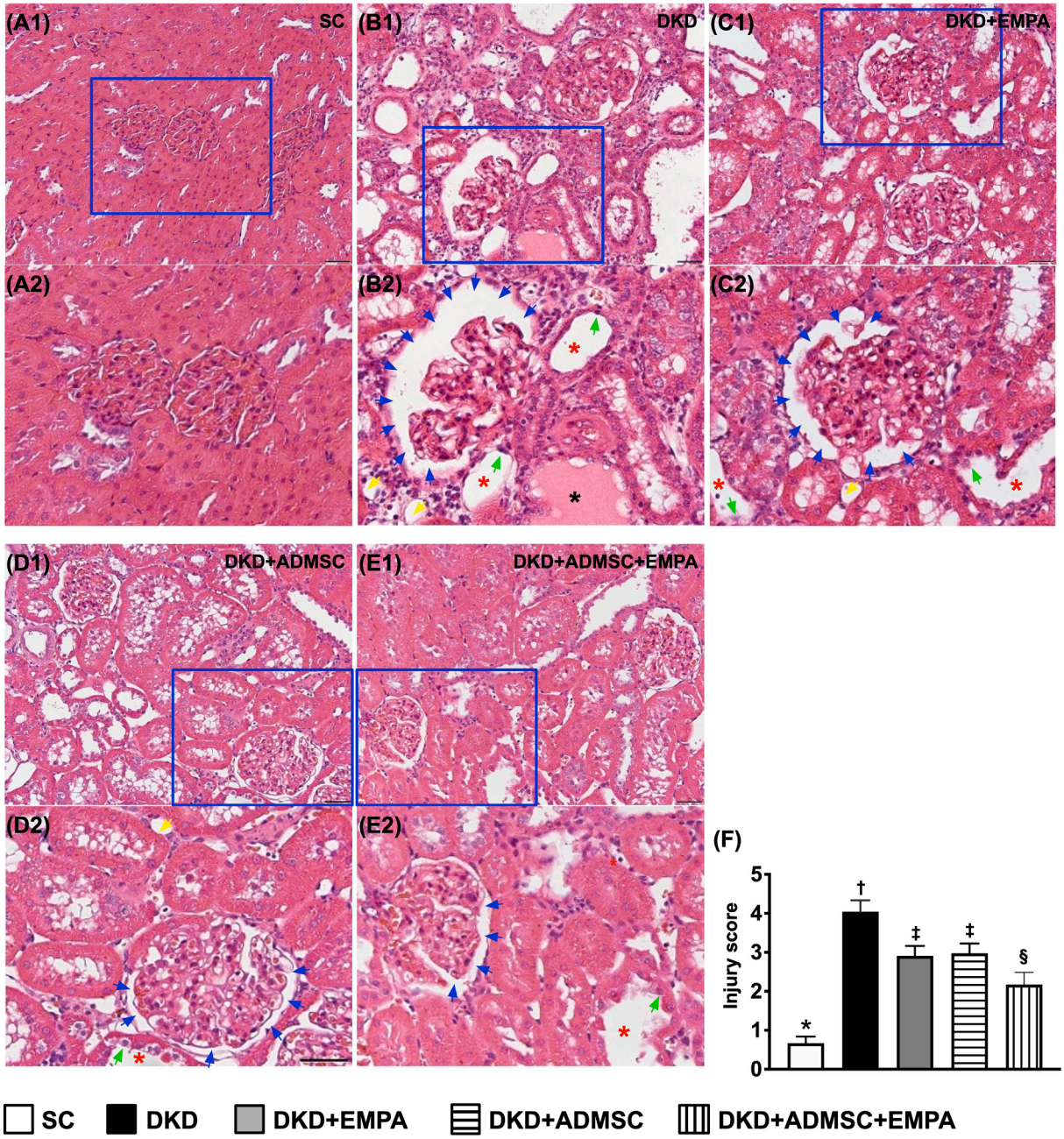

Fig. 3. Impact of ADMSCs-EMPA therapy on attenuating the kidney injury score by day 60 after CKD induction (A1 to E1) Light microscopic findings (200x; H&E stain) illustrating the remarkably increased loss of brush border in renal tubules (yellow arrows), tubular necrosis (green arrows), tubular dilatation (red asterisk), protein cast formation (black asterisk), and dilatation of Bowman's capsule (blue arrows) in DKD group than in other groups. All scale bars in the lower right corner represent 50 μm. **(A2 to E2)** Showing the magnified blue square box for observing the more clear kidney ultrastructure. **(F)** Analytical result of kidney injury score, * vs. other groups with different symbols (†, ‡, §), $p < 0.0001$. All statistical analyses were performed by one-way ANOVA, followed by Bonferroni multiple comparison post hoc test (n = 6 for each group). Symbols (*, †, ‡, §) indicate significance (at 0.05 level).
Abbreviations: CKD : chronic kidney disease; BUN : blood urea nitrogen; SC : sham-operated control; DKD : diabetic kidney disease; EMPA : empagliflozin; ADMSC: adipose-derived mesenchymal stem cell.

being conducted), these three parameters were lowest in SC group, highest in group 2, and significantly lower in group 5 than in groups 3 and 4. Still, they showed no difference between these latter two groups [Fig. 1G, K, O].

The time courses of renal artery resistive index (RARI) among the groups

The time courses of renal artery RI among the groups were shown in [Fig. 2]. By day 0, the renal artery RI did not differ among the five groups. However, by day 14 after CKD induction, this parameter was significantly higher in groups 2 to 5 than that of the SC group.

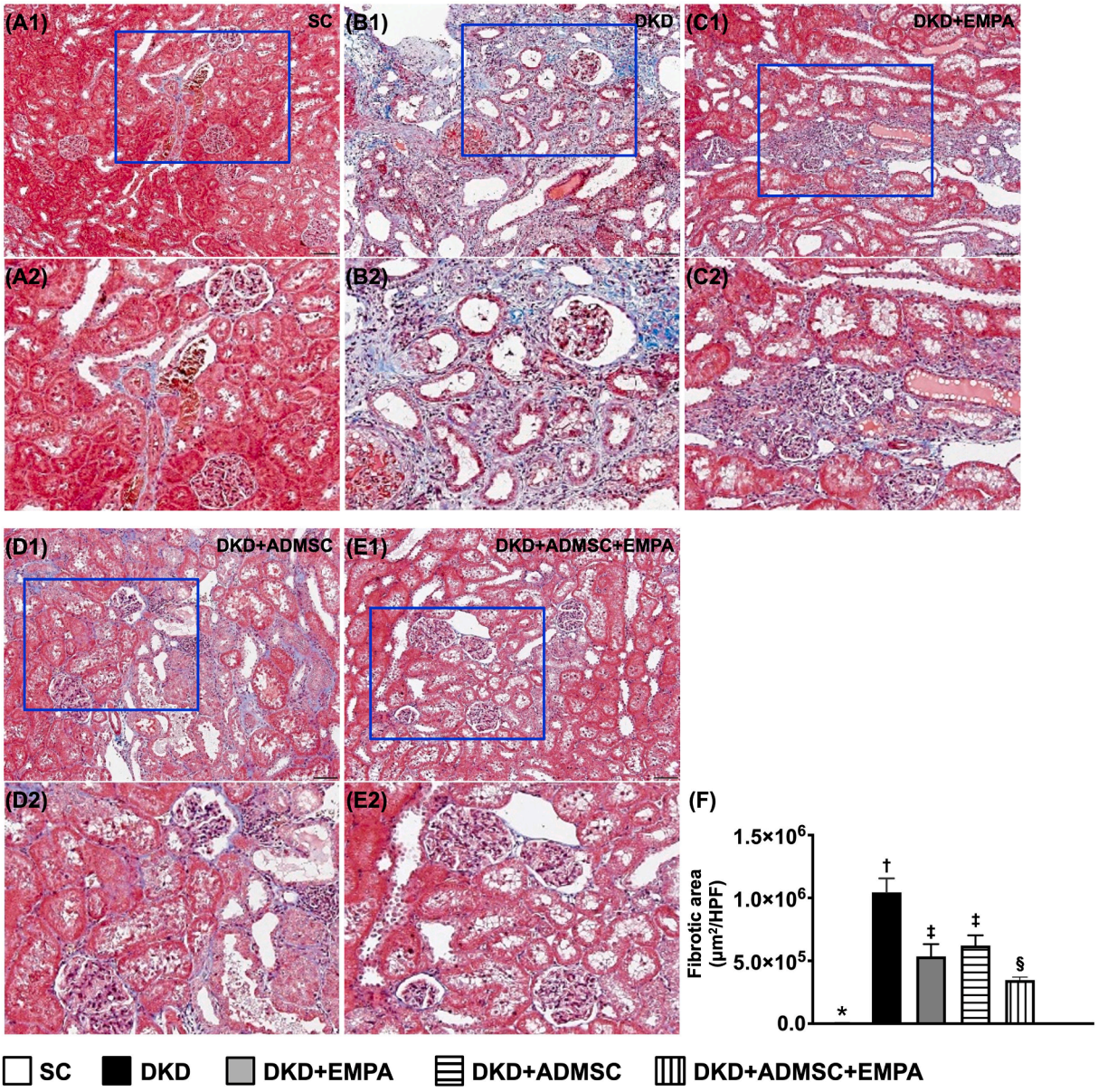

Fig. 4. Impact of ADMSCs-EMPA therapy on alleviating fibrosis in renal tissue by day 60 after CKD induction (A1 to E1) Demonstrating the microscopic finding of Masson's trichrome stain (200x) for verification of fibrosis in kidney parenchyma (blue color). All scale bars in the lower right corner represent 50 μm. (**A2 to E2**) Exhibiting the magnified blue square box for inspecting kidney ultrastructure more clearly. (**F**) Analytical result of fibrotic area, * vs. other groups with different symbols (†, ‡, §), $p < 0.0001$. All statistical analyses were performed by one-way ANOVA, followed by Bonferroni multiple comparison post hoc test ($n = 6$ for each group). Symbols (*, †, ‡, §) indicate significance (at 0.05 level).
Abbreviations: CKD : chronic kidney disease; SC : sham-operated control; DKD : diabetic kidney disease; EMPA : empagliflozin; ADMSC : adipose-derived mesenchymal stem cell.

Additionally, by day 28 after CKD induction, this parameter was lowest in the SC group, significantly lower in groups 3 and 5 than in groups 2 and 4, but it demonstrated no difference between the groups 2 and 4 or between the groups 3 and 5. Furthermore, by day 60 after CKD induction, this parameter was also lowest in the SC group, highest in group 2, and significantly lower in group 5 than in groups 3 and 4. Still, it was similar between these latter two groups.

Impact of ADMSCs-EMPA therapy on attenuating the kidney injury score, fibrotic area, and oxidative stress in kidney parenchyma by day 60 after CKD induction

To elucidate whether ADMSCs-EMPA therapy would protect the integrity of kidney architecture, histopathological findings were performed in kidney specimens. The H.E. stain of microscopic histopathological evaluation illustrated that the kidney injury score [Fig. 3] (i.e., the parameters summarized as the scoring of tubular necrosis, loss of brush border, cast formation, Bowman's capsule, and tubular dilatation) was the most significantly increased in group 2 as compared with the SC group, significantly reduced in group 5 than in groups 3 and 4, but it exhibited no difference between groups 3 and 4 [Fig. 3].

When we looked at the Masson's trichrome stain, we found that the fibrotic area of the kidney parenchyma revealed a similar manner of kidney injury score among the groups [Fig. 4].

When we further scrutinized the immunohistochemical (IHC) microscopic examination, we identified that the scoring of positively stained 8-OHdG, an index of cellular level of oxidative stress, also identically resembled the pattern of kidney injury score among the five

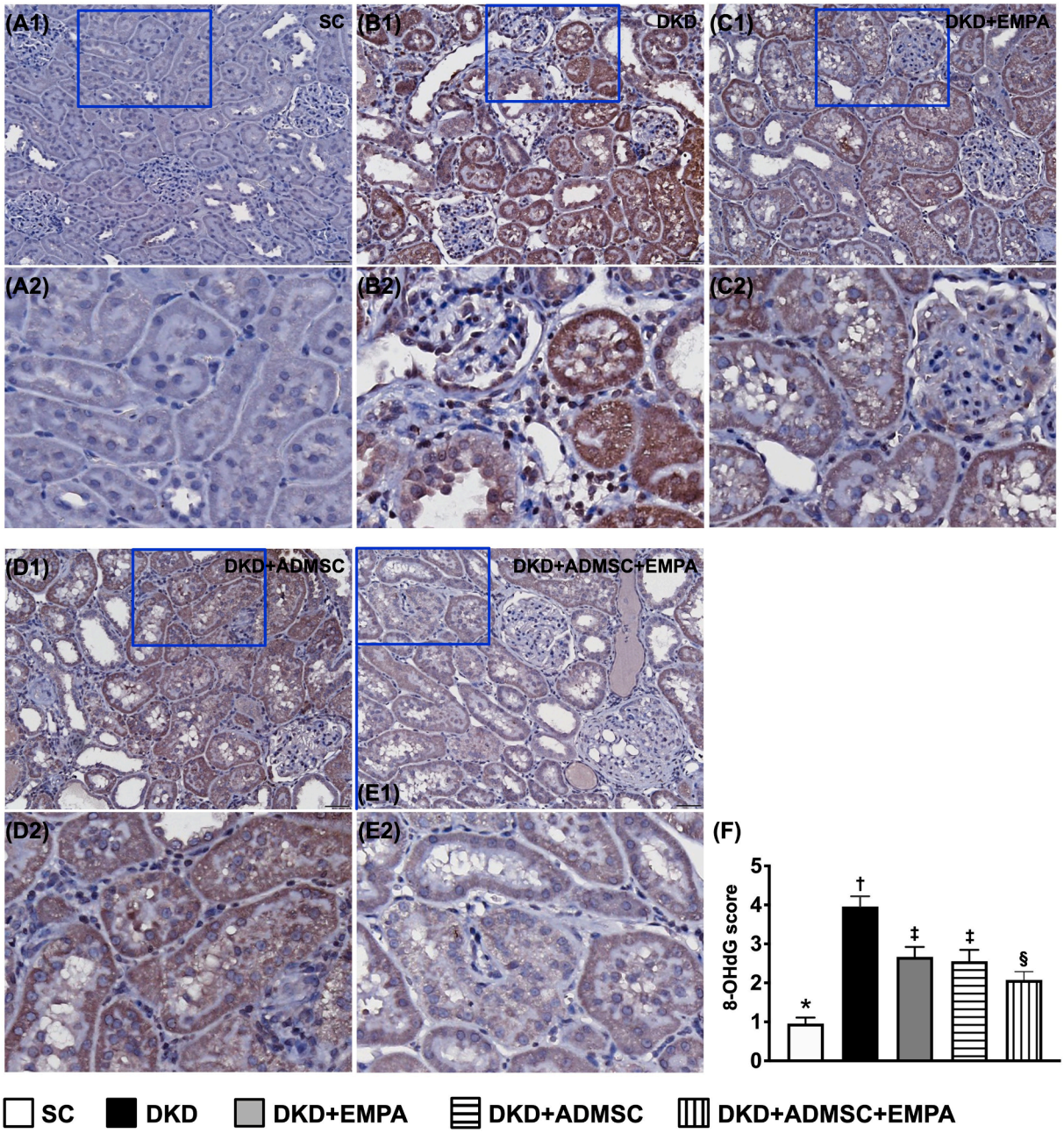

Fig. 5. Impact of ADMSCs-EMPA therapy on ameliorating oxidative stress in renal tissue by day 60 after CKD induction (A1 to E1) Displaying the microscopic finding (200x) of 8-OHdG stain for recognizing the intensity of oxidative stress expression. All scale bars in the lower right corner represent 50 μm. **(A2 to E2)** Exhibiting the magnified blue square box for inspecting more clearly oxidative-stress expression in renal tubules. **(F)** Analytical result of expression of the 8-OHdG score, * vs. other groups with different symbols (†, ‡, §), $p < 0.0001$. All statistical analyses were performed by one-way ANOVA, followed by Bonferroni multiple comparison post hoc test (n = 6 for each group). Symbols (*, †, ‡, §) indicate significance (at 0.05 level).
Abbreviations: CKD : chronic kidney disease; SC : sham-operated control; DKD : diabetic kidney disease; EMPA : empagliflozin; ADMSC : adipose-derived mesenchymal stem cell.

groups [Fig. 5]. Therefore, the findings from [Figs. 3–5] implicated that ADMSCs facilitated the effect of EMPA on protecting the ultrastructure of kidney parenchyma in the setting of DKD rodent.

The histopathological analyses of kidney injury molecule and podocyte components in kidney parenchyma by day 60 after CKD induction

To specifically observe the ultrastructural damage of glomeruli and renal tubules, the immunofluorescent (IF) microscope was utilized in the present study. As we expected, the fluorescent intensity of positively stained KIM-1, predominantly localized in renal tubules, was the most significantly expressed in group 2, the most oppositely represented in SC group (i.e., group 1) as compared to group 2 and significantly reduced in group 5 than in groups 3 and 4, but it revealed no difference in groups 3 and 4 [Supplementary Fig. 2].

Next, when focused on the glomerulus microstructure, we discovered that the cellular expressions of ZO-1 and synaptopodin, two components of podocytes predominantly situated in the glomeruli, disclosed a contrary manner of KIM-1 among the groups [Fig. 6]. These findings could, at least in part, explain why the proteinuria was substantially ameliorated in DKD animals after receiving ADMSCs-EMPA treatment.

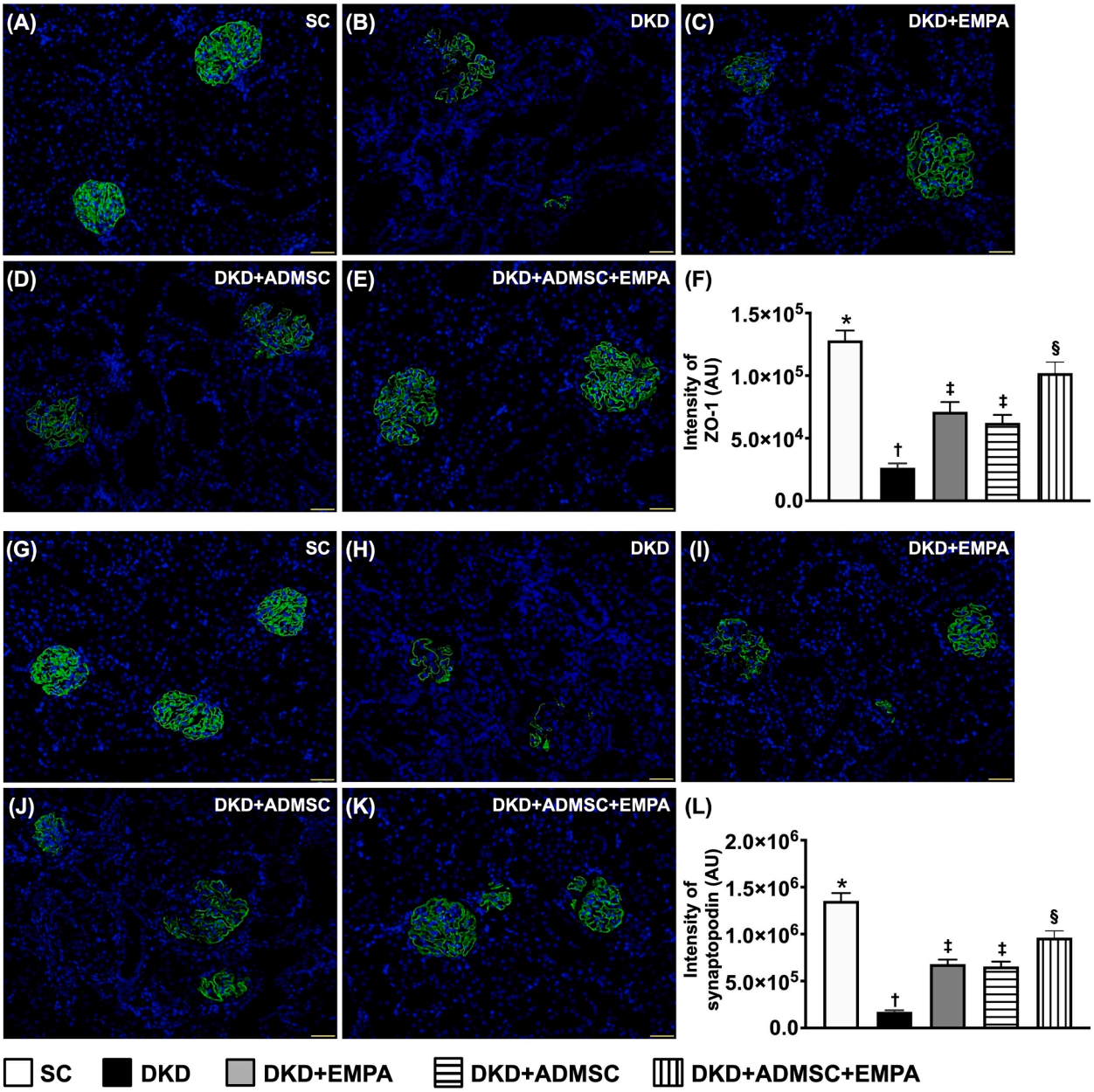

Fig. 6. Impact of ADMSCs-EMPA therapy on preserving the podocyte components in kidney parenchyma by day 60 after CKD induction (A to E) Demonstrating the immunofluorescent (IF) microscopic finding (200x) for identification of the expression of ZO-1 (green color). **(F)** Analytical result of the expression of ZO-1, * vs. other groups with different symbols (†, ‡, §), $p < 0.0001$. **(G to K)** Demonstrating the IF microscopic finding (200x) for identification of the expression of synaptopodin (green color). **(L)** Analytical result of the expression of synaptopodin, * vs. other groups with different symbols (†, ‡, §), $p < 0.0001$. All scale bars in the lower right corner represent 50 μm. All statistical analyses were performed by one-way ANOVA, followed by Bonferroni multiple comparison post hoc test (n = 6 for each group). Symbols (*, †, ‡, §) indicate significance (at 0.05 level).
Abbreviations: CKD : chronic kidney disease; SC : sham-operated control; DKD : diabetic kidney disease; EMPA : empagliflozin; ADMSC : adipose-derived mesenchymal stem cell.

The protein levels of apoptosis, fibrosis, damaged and autophagic biomarkers in kidney parenchyma by day 60 after CKD induction

To clarify the protein levels of apoptotic and fibrotic biomarkers, the Western blot analysis was employed. The result disclosed that three parameters of apoptosis, including protein expressions of cleaved caspase 3, cleaved PARP and mitochondrial Bax [Fig. 7A–C], as well as two parameters of fibrosis, including TGF-β and p-Smad 3 [Fig. 7D and E], were highest in group 2, lowest in SC group, and significantly lower in group 5 than in groups 3 and 4. In contrast, the protein expressions of p-Smad 1/5 and BMP-2 disclosed a contrary manner of TGF-β among 5 groups [Fig. 7F and G].

To delineating the therapeutic impact of ADMSCs-EMPA on reducing mitochondrial/DNA damaged and autophagic expressions, the Western blot analysis once more was employed in the current study. The result demonstrated that the protein levels of p22 phox and p-DRP1, two parameters of mitochondrial damage, protein expression of γ-H2AX, an index of DNA-injured biomarker, and protein expression of Atg 5, an indicator of autophagy, were lowest in SC group, highest in group 2 and significantly lower in group 5 than in groups 3 and 4 [Fig. 7H–K].

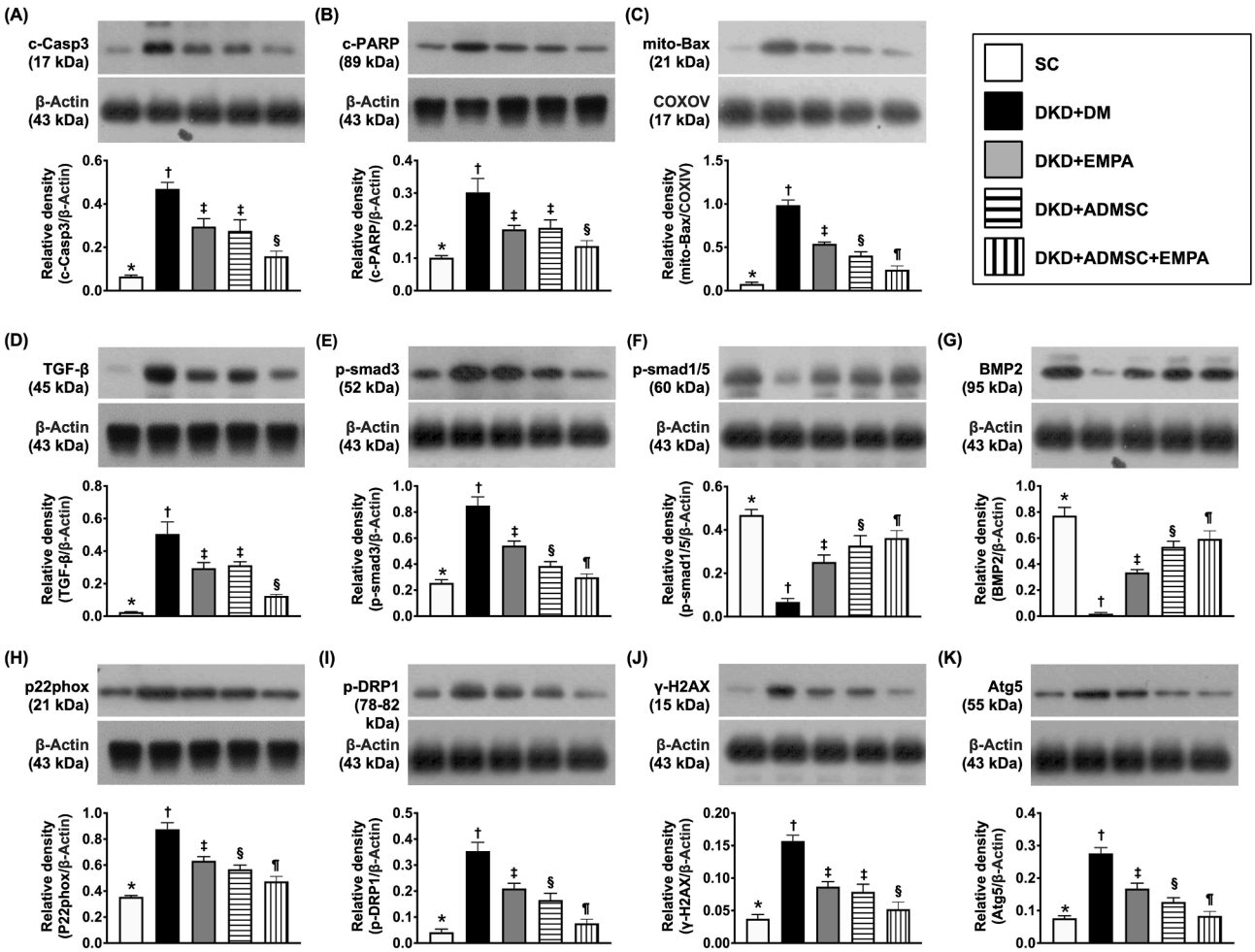

Fig. 7. Impact of ADMSCs-EMPA therapy on attenuating the protein levels of apoptosis, fibrosis, damaged and autophagic biomarkers in renal tissue by day 60 after CKD induction (A) Protein level of cleaved caspase 3 (c-Casp 3), * vs. other groups with different symbols (†, ‡, §), $p < 0.0001$. **(B)** Protein level of cleaved Poly (ADP-ribose) polymerase (PARP), * vs. other groups with different symbols (†, ‡, §), $p < 0.0001$. **(C)** Protein level of mitochondrial Bax (mit-Bax), * vs. other groups with different symbols (†, ‡, §, ¶), $p < 0.0001$. **(D)** Protein expression of transforming growth factor (TGF-β), * vs. other groups with different symbols (†, ‡, §), $p < 0.0001$. **(E)** Protein level of phosphorylated (p)-Smad 3, * vs. other groups with different symbols (†, ‡, §, ¶), $p < 0.0001$. **(F)** Protein level of p-Smad 1/5, * vs. other groups with different symbols (†, ‡, §, ¶), $p < 0.0001$. **(G)** Protein level of bone morphogenetic protein 2 (BMP-2), * vs. other groups with different symbols (†, ‡, §, ¶), $p < 0.0001$. **(H)** Protein levels of p22 phox. **(I)** Protein level of phosphorylation of dynamin-related protein 1 (p-DRP1), * vs. other groups with different symbols (†, ‡, §, ¶), $p < 0.0001$. **(J)** Protein level of γ-H2AX, * vs. other groups with different symbols (†, ‡, §), $p < 0.0001$. **(K)** Protein level of Atg 5, * vs. other groups with different symbols (†, ‡, §, ¶), $p < 0.0001$. All statistical analyses were performed by one-way ANOVA, followed by Bonferroni multiple comparison post hoc test (n = 6 for each group). Symbols (*, †, ‡, §, ¶) indicate significance (at 0.05 level).
Abbreviations: CKD : chronic kidney disease; SC : sham-operated control; DKD : diabetic kidney disease; EMPA : empagliflozin; ADMSC : adipose-derived mesenchymal stem cell.

The protein levels of oxidative stress and inflammation in kidney parenchyma by day 60 after CKD induction

An association between DKD and the upregulation of oxidative stress and inflammation has been well recognized. In this study, we intended to delineate whether the ADMSCs-EMPA therapy would alleviate these molecular perturbations. Western blot analysis was used again. The result declared that the protein levels of NOX-1, NOX-2, and oxidized protein, three parameters of oxidative stress, were greatly increased in group 2 as compared to that of the SC group, and significantly reduced in groups 5 than in groups 3 and 4 [Fig. 8A–C]. Additionally, the protein expressions of p–NF–κB, TNF-α, and MMP-9, three inflammation parameters, divulged a contrary manner of NOX-1 among the groups [Fig. 8D–F].

Discussion

This study which explored the therapeutic effect of AMDSCs-EMPA on safeguarding the residual kidney function and ultrastructural integrity of the kidney in the setting of DKD delivered several noticeable connotations. First, we successfully created a DKD animal model that not only mimicked the clinical DKD setting but also provided a platform for pharmacological and biological studies as well as investigating the mechanistic basis of DKD. Second, the result of the present study demonstrated that combined ADMSCs and EMPA was superior to merely either one in preserving the functional and architectural integrities of kidney in DKD rodent. This finding might implicate that ADMSCs could facilitate the therapeutic impact of EMPA, i.e., defined as "added on beneficial effects" on protecting the kidney in DKD rodents. Third, based on the findings in the present study, we concluded that hyperglycemia damaged the kidney function and its microstructures mainly through several signaling pathways, including fibrosis, oxidative stress, inflammatory reaction, and autophagy.

It is globally well-known that hyperglycemia commonly worsens renal function in most CKD patients [1,3,4], ultimately advancing to ESRD [5]. One important finding in the present study was that, as

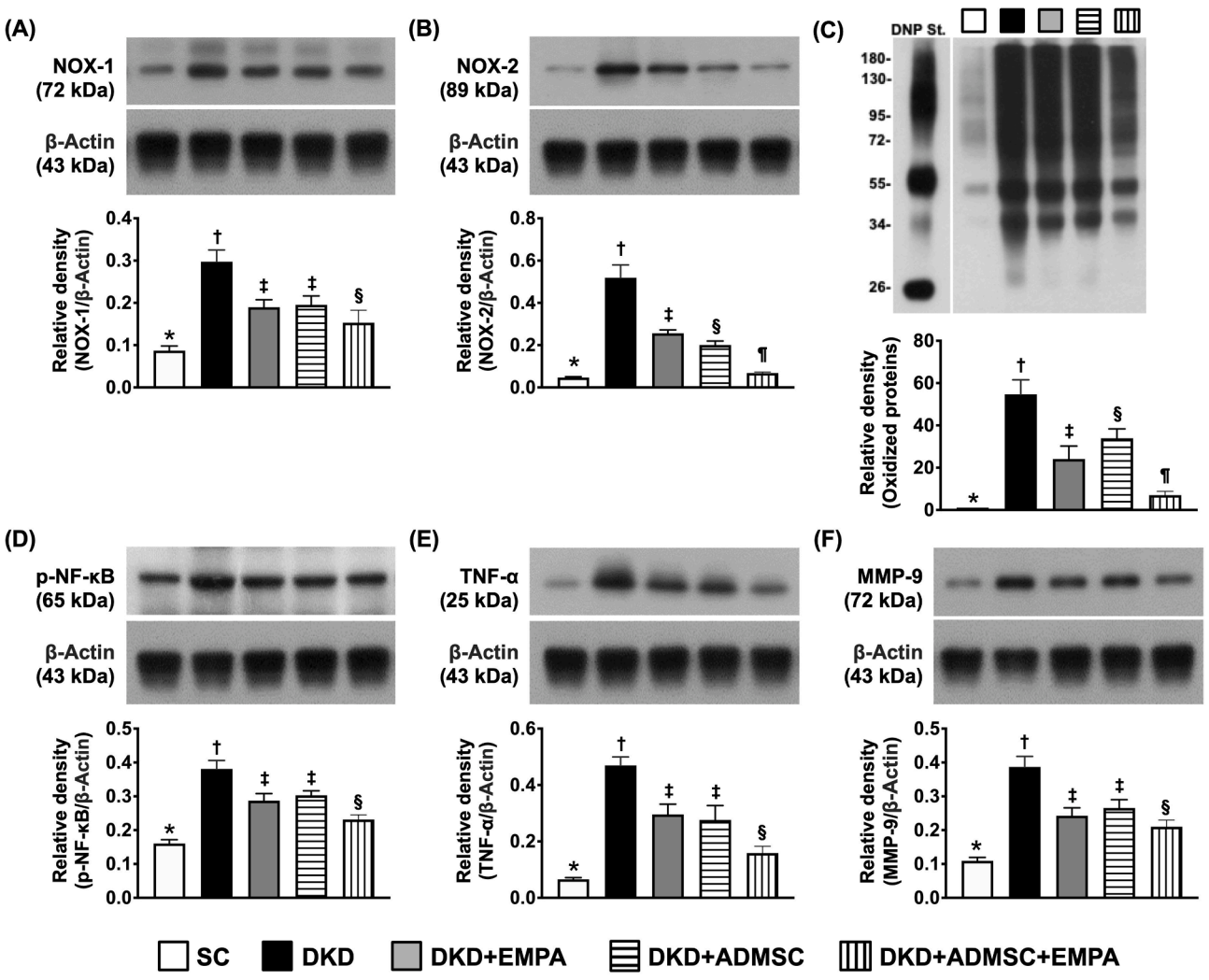

Fig. 8. Impact of ADMSCs-EMPA therapy on downregulating the protein levels of oxidative stress and inflammation in renal tissue by day 60 after CKD induction (A) Protein level of NOX-1, * vs. other groups with different symbols (†, ‡, §), $p < 0.0001$. **(B)** Protein level of NOX-2, * vs. other groups with different symbols (†, ‡, §, ¶), $p < 0.0001$. **(C)** The oxidized protein level, * vs. other groups with different symbols (†, ‡, §, ¶), $p < 0.0001$. Left and right lanes expressed on the upper panel indicated the molecular weight marker and control oxidized molecular protein standard, respectively). M.W. = molecular weight; DNP = 1–3 dinitrophenylhydrazone. **(D)** Protein level of phosphorylated nuclear factor (p–NF)–κB, * vs. other groups with different symbols (†, ‡, §), $p < 0.0001$. **(E)** Protein level of tumor necrosis factor (TNF)-α, * vs. other groups with different symbols (†, ‡, §), $p < 0.0001$. **(F)** Protein level of matrix metalloproteinase (MMP-9), * vs. other groups with different symbols (†, ‡, §), $p < 0.0001$. All statistical analyses were performed by one-way ANOVA, followed by Bonferroni multiple comparison post hoc test (n = 6 for each group). Symbols (*, †, ‡, §, ¶) indicate significance (at 0.05 level).
Abbreviations: CKD : chronic kidney disease; SC : sham-operated control; DKD : diabetic kidney disease; EMPA : empagliflozin; ADMSC : adipose-derived mesenchymal stem cell.

compared with the SC, the renal function in CKD was notably reduced by day 14 after CKD induction that was even more deteriorated by day 28 after CKD induction, which corresponded to the time point of day 21 after STZ treatment, i.e., that time interval of already successfully created DKD in rodent. Our finding, in addition to being consistent with the findings from the previous studies, once again proved that persistent hyperglycemia undoubtedly deteriorated the residual renal function in the CKD setting.

Plentiful evidence from clinical trials [13–15] and animal model studies [17]has demonstrated that SGLT2 inhibitors effectively protected the residual renal function in the DKD setting. Additionally, numerous data [26,27,29,31,32] have proved that cell therapy, especially those of MSCs, effectively protects the renal function in CKD setting. An essential finding in the present study was that not only AMDSCs but also EMPA therapy effectively protected the residual renal function in DKD animals, i.e., preventing the upregulations of circulatory levels of BUN and creatinine and the ratio of urine protein to urine creatinine. In this way, our findings were consistent with the findings of previous studies [26,27,29,31,32]. Surprisingly, while the positive impact of ADMSCs and EMPA therapy on protecting kidney function in CKD or DKD settings is still lacking adequate evidence to address whether combined ADMSC and EMPA therapy would offer a synergic effect for further improving renal function in DKD settings. The most critical finding in the present study was that combined ADMSCs and EMPA therapy was superior to either one treatment, i.e., bolstering our purpose to prove that “ADMSCs had additional beneficial effects to empagliflozin on protecting renal function”. Accordingly, our innovative finding may deliver a potentially clinical message for the possible utilization of this strategic management for DKD patients without ethical issues, especially in those who are already refractory to traditional therapy.

It is well recognized that the functional integrity of podocyte components in glomeruli plays a crucial role in avoiding protein leakage from glomeruli, impeding proteinuria [17,31]. In the present study, the

podocyte components were significantly reduced. In contrast, the kidney injury molecule-1 was significantly increased in DKD animals as compared with the SC that was remarkably reversed by in ADMSCs or EMPA treatment and further remarkably reversed in those of DKD animals after receiving combined ADMSCs and EMPA regimen. These findings, in addition to corroborating with the finding of previous studies [17,31], could, at least in part, explain why the ratio of urine protein to urine creatinine was substantially reduced with than without ADMSCs-EMPA treatment.

Link between CKD and eliciting of oxidative stress, inflammation and fibrosis has been well understood in CKD/DKD settings [26,27,29,31,32]. A principal finding in the present study was that all of the molecular-cellular perturbations, including oxidative stress, inflammatory, fibrotic, DNA-damaged and autophagic biomarkers, were notably increased in DKD animals as compared with SC animals that were significantly suppressed by ADMSCs or EMPA treatment and further significantly suppressed by these therapeutic components. In this way, our findings, in addition to strengthening the findings of the previous studies [26,27,29,31,32], could partially vindicate why the urine protein and kidney injury score were markedly alleviated by ADMSCs-EMPA therapy.

Physiologically, the renal tubules commonly rely on adequate oxidative ability (i.e., through oxidation phosphorylation) to connive the active transport of glucose and molecules [39–42]. In this way, plentiful mitochondria in the tubules are required to meet the energetic requirement, making mitochondrial susceptible to oxidative-stress damage [39–42]. Additionally, a study has previously revealed that 8-OHdG plays a critical role in oxidative stress [43]. A cardinal finding in the present study was that 8-OHdG expression, which was identified dominantly in renal tubules [referred to Fig. 5], i.e., vigorous oxidative stress, was substantially enhanced in DKD animals. Our finding, in addition to being supported by the previous studies [39–43], could once again explain why the renal tubules were more susceptible to hyperglycemic damage in DKD animals without than with ADMSCs-EMPA treatment.

Study limitation

Our study may have some limitations. First, although the study had done extensive work, the exact underlying mechanism regarding how the ADMSCs-EMPA treatment improved the outcomes had not been fully investigated. Second, despite the study period being 60 days, it might still not be enough to investigate the more long-term unfavorable outcomes of hyperglycemia-induced renal complications in CKD rodents. Third, if the study further enrolled the CKD only control, the progression of renal injury and the protective impacts of DAPA and ADMSCs could be delineated not only in the DKD but also in the CKD setting. In this way, the pathophysiology of diabetes-mediated CKD and the specific potential of DAPA-ADMSCs therapy for DKD could also be clarified in the present study.

Conclusion

In conclusion, the results of our study demonstrated that ADMSCs would add to beneficial effects of EMPA on preserving the residual renal function and integrity of kidney architecture in DKD rats.

Conflicts of interest

The authors have no conflicts of interest to declare.

Acknowledgment

This project was supported by the program grant from Chang Gung Memorial Hospital, Taiwan; Chang Gung University, Taiwan (CMRPG8L0211).

Appendix A. Supplementary data

Supplementary data to this article can be found online at https://doi.org/10.1016/j.bj.2023.100613.

References

[1] Glassock RJ, Warnock DG, Delanaye P. The global burden of chronic kidney disease: estimates, variability and pitfalls. Nat Rev Nephrol 2017;13(2):104–14.
[2] Guideline. Sugars intake for adults and children. 2015. Geneva.
[3] Global Burden of Disease Study C. Global, regional, and national incidence, prevalence, and years lived with disability for 301 acute and chronic diseases and injuries in 188 countries, 1990-2013: a systematic analysis for the Global Burden of Disease Study 2013. Lancet 2015;386(9995):743–800.
[4] Alicic RZ, Rooney MT, Tuttle KR. Diabetic kidney disease: challenges, progress, and possibilities. Clin J Am Soc Nephrol 2017;12(12):2032–45.
[5] Tsai MH, Hsu CY, Lin MY, Yen MF, Chen HH, Chiu YH, et al. Incidence, prevalence, and duration of chronic kidney disease in taiwan: results from a community-based screening program of 106,094 individuals. Nephron 2018;140(3):175–84.
[6] Patschan D, Muller GA. Acute kidney injury in diabetes mellitus. Internet J Nephrol 2016;2016:6232909.
[7] Muskiet MH, Smits MM, Morsink LM, Diamant M. The gut-renal axis: do incretin-based agents confer renoprotection in diabetes? Nat Rev Nephrol 2014;10(2):88–103.
[8] Persson P, Hansell P, Palm F. Tubular reabsorption and diabetes-induced glomerular hyperfiltration. Acta Physiol 2010;200(1):3–10.
[9] Stehouwer CDA. Microvascular dysfunction and hyperglycemia: a vicious cycle with widespread consequences. Diabetes 2018;67(9):1729–41.
[10] Kidokoro K, Cherney DZI, Bozovic A, Nagasu H, Satoh M, Kanda E, et al. Evaluation of glomerular hemodynamic function by empagliflozin in diabetic mice using in vivo imaging. Circulation 2019;140(4):303–15.
[11] Cherney DZ, Perkins BA, Soleymanlou N, Maione M, Lai V, Lee A, et al. Renal hemodynamic effect of sodium-glucose cotransporter 2 inhibition in patients with type 1 diabetes mellitus. Circulation 2014;129:587–97.
[12] Chu C, Lu YP, Yin L, Hocher B. The SGLT2 inhibitor empagliflozin might be a new approach for the prevention of acute kidney injury. Kidney Blood Press Res 2019;44(2):149–57.
[13] Neal B, Perkovic V, Mahaffey KW, de Zeeuw D, Fulcher G, Erondu N, et al. Canagliflozin and cardiovascular and renal events in type 2 diabetes. N Engl J Med 2017;377(21):644–57.
[14] Verma S, Mazer CD, Yan AT, Mason T, Garg V, Teoh H, et al. Effect of empagliflozin on left ventricular mass in patients with type 2 diabetes mellitus and coronary artery disease: the EMPA-HEART cardiolink-6 randomized clinical trial. Circulation 2019;140(21):1693–7102.
[15] Zelniker TA, Bonaca MP, Furtado RHM, Mosenzon O, Kuder JF, Murphy SA, et al. Effect of dapagliflozin on atrial fibrillation in patients with type 2 diabetes mellitus: insights from the DECLARE-TIMI 58 trial. Circulation 2020;141(15):1227–34.
[16] Dekkers CCJ, Petrykiv S, Laverman GD, Cherney DZ, Gansevoort RT, Heerspink HJL. Effects of the SGLT-2 inhibitor dapagliflozin on glomerular and tubular injury markers. Diabetes Obes Metabol 2018;20(8):1988–93.
[17] Yang CC, Chen YT, Wallace CG, Chen KH, Cheng BC, Sung PH, et al. Early administration of empagliflozin preserved heart function in cardiorenal syndrome in rat. Biomed Pharmacother 2019;109:658–70.
[18] Barutta F, Bernardi S, Gargiulo G, Durazzo M, Gruden G. SGLT2 inhibition to address the unmet needs in diabetic nephropathy. Diabetes Metab Res Rev 2019;35(7):e3171.
[19] Li X, Michaeloudes C, Zhang Y, Wiegman CH, Adcock IM, Lian Q, et al. Mesenchymal stem cells alleviate oxidative stress-induced mitochondrial dysfunction in the airways. J Allergy Clin Immunol 2018;141(5):1634–45.
[20] Song IH, Jung KJ, Lee TJ, Kim JY, Sung EG, Bae YC, et al. Mesenchymal stem cells attenuate adriamycin-induced nephropathy by diminishing oxidative stress and inflammation via downregulation of the NF-kB. Nephrology 2018;23(5):483–92.
[21] Chen KH, Hsiao HY, Glenn Wallace C, Lin KC, Li YC, Huang TH, et al. Combined adipose-derived mesenchymal stem cells and low-energy extracorporeal shock wave therapy protect the brain from brain death-induced injury in rat. J Neuropathol Exp Neurol 2019;78(1):65–77.
[22] Jung KJ, Lee GW, Park CH, Lee TJ, Kim JY, Sung EG, et al. Mesenchymal stem cells decrease oxidative stress in the bowels of interleukin-10 knockout mice. Gut Liver 2020;14(1):100–7.
[23] Lin KC, Yeh JN, Chen YL, Chiang JY, Sung PH, Lee FY, et al. Xenogeneic and allogeneic mesenchymal stem cells effectively protect the lung against ischemia-reperfusion injury through downregulating the inflammatory, oxidative stress, and autophagic signaling pathways in rat. Cell Transplant 2020;29. 963689720954140.
[24] Chen YT, Chuang FC, Yang CC, Chiang JY, Sung PH, Chu YC, et al. Combined melatonin-adipose derived mesenchymal stem cells therapy effectively protected the testis from testicular torsion-induced ischemia-reperfusion injury. Stem Cell Res Ther 2021;12(1):370.
[25] Yin TC, Li YC, Sung PH, Chiang JY, Shao PL, Yip HK, et al. Adipose-derived mesenchymal stem cells overexpressing prion improve outcomes via the NLRP3 inflammasome/DAMP signalling after spinal cord injury in rat. J Cell Mol Med 2023;27(4):482–95.

[26] Yun CW, Lee SH. Potential and therapeutic efficacy of cell-based therapy using mesenchymal stem cells for acute/chronic kidney disease. Int J Mol Sci 2019;20(7):1619.
[27] Yang CC, Sung PH, Cheng BC, Li YC, Chen YL, Lee MS, et al. Safety and efficacy of intrarenal arterial autologous CD34+ cell transfusion in patients with chronic kidney disease: a randomized, open-label, controlled phase II clinical trial. Stem Cells Transl Med 2020;9(8):827–38.
[28] Lin KC, Yip HK, Shao PL, Wu SC, Chen KH, Chen YT, et al. Combination of adipose-derived mesenchymal stem cells (ADMSC) and ADMSC-derived exosomes for protecting kidney from acute ischemia-reperfusion injury. Int J Cardiol 2016;216:173–85.
[29] Ko SF, Chen KH, Wallace CG, Yang CC, Sung PH, Shao PL, et al. Protective effect of combined therapy with hyperbaric oxygen and autologous adipose-derived mesenchymal stem cells on renal function in rodent after acute ischemia-reperfusion injury. Am J Transl Res 2020;12(7):3272–87.
[30] Sung PH, Chiang HJ, Chen CH, Chen YL, Huang TH, Zhen YY, et al. Combined therapy with adipose-derived mesenchymal stem cells and ciprofloxacin against acute urogenital organ damage in rat sepsis syndrome induced by intrapelvic injection of cecal bacteria. Stem Cells Transl Med 2016;5(6):782–92.
[31] Yip HK, Lee MS, Sun CK, Chen KH, Chai HT, Sung PH, et al. Therapeutic effects of adipose-derived mesenchymal stem cells against brain death-induced remote organ damage and post-heart transplant acute rejection. Oncotarget 2017;8(65):108692–711.
[32] Chen KH, Chai HT, Lin KC, Chiang JY, Sung PH, Chen CH, et al. Dose-dependent benefits of iron-magnetic nanoparticle-coated human umbilical-derived mesenchymal stem cell treatment in rat intracranial hemorrhage model. Stem Cell Res Ther 2022;13(1):265.
[33] Yang CC, Sung PH, Chen KH, Chai HT, Chiang JY, Ko SF, et al. Valsartan- and melatonin-supported adipose-derived mesenchymal stem cells preserve renal function in chronic kidney disease rat through upregulation of prion protein participated in promoting PI3K-Akt-mTOR signaling and cell proliferation. Biomed Pharmacother 2022;146:112551.
[34] Yue Y, Yeh JN, Chiang JY, Sung PH, Chen YL, Liu F, et al. Intrarenal arterial administration of human umbilical cord-derived mesenchymal stem cells effectively preserved the residual renal function of diabetic kidney disease in rat. Stem Cell Res Ther 2022;13(1):186.
[35] Tajiri Y, Moller C, Grill V. Long-term effects of aminoguanidine on insulin release and biosynthesis: evidence that the formation of advanced glycosylation end products inhibits B cell function. Endocrinology 1997;138(1):273–80.
[36] Yang CC, Sung PH, Chiang JY, Chai HT, Chen CH, Chu YC, et al. Combined tacrolimus and melatonin effectively protected kidney against acute ischemia-reperfusion injury. Faseb J 2021;35(6):e21661.
[37] Li YC, Chen CH, Chang CL, Chiang JY, Chu CH, Chen HH, et al. Melatonin and hyperbaric oxygen therapies suppress colorectal carcinogenesis through pleiotropic effects and multifaceted mechanisms. Int J Biol Sci 2021;17(14):3728–44.
[38] Li YC, Sung PH, Yang YH, Chiang JY, Yip HK, Yang CC. Dipeptidyl peptidase 4 promotes peritoneal fibrosis and its inhibitions prevent failure of peritoneal dialysis. Commun Biol 2021;4(1):144.
[39] Sancho-Martinez SM, Lopez-Novoa JM, Lopez-Hernandez FJ. Pathophysiological role of different tubular epithelial cell death modes in acute kidney injury. Clin Kidney J 2015;8(5):548–59.
[40] Linkermann A, Chen G, Dong G, Kunzendorf U, Krautwald S, Dong Z. Regulated cell death in AKI. J Am Soc Nephrol 2014;25(12):2689–701.
[41] Bhargava P, Schnellmann RG. Mitochondrial energetics in the kidney. Nat Rev Nephrol 2017;13(10):629–46.
[42] Clark AJ, Parikh SM. Mitochondrial metabolism in acute kidney injury. Semin Nephrol 2020;40(2):101–13.
[43] Valavanidis A, Vlachogianni T, Fiotakis C. 8-hydroxy-2' -deoxyguanosine (8-OHdG): a critical biomarker of oxidative stress and carcinogenesis. J Environ Sci Health C Environ Carcinog Ecotoxicol Rev 2009;27(2):120–39.